

Design of Interleaved Converter with Adaptive SOC Control

J Uday Venkatesh

Department of Electrical and
Electronics Engineering,
ANITS, Visakhapatnam,
Andhra Pradesh 531162, India.

S.J.V Prakesh

Department of Electrical and
Electronics Engineering,
ANITS, Visakhapatnam,
Andhra Pradesh 531162, India.

L Vijay

Department of Electrical and
Electronics Engineering,
ANITS, Visakhapatnam,
Andhra Pradesh 531162, India.

ABSTRACT

The configuration of the proposed converter not only reduces the current stress but also constrains the input current ripple, which decreases the conduction losses and lengthens the life time of the input source. In addition, due to the loss less passive clamp performance, leakage energy is recycled to the output terminal. Hence, large voltage spikes across the main switches are alleviated, and the efficiency is improved. Even the low voltage stress makes the low-voltage-rated MOSFETs be adopted for reductions of conduction losses and cost. An additional battery control is added to the input renewable energy system to work as a back up storage system with reduces the variations in the output waveform.

Keywords: interleaved converter, solar, Battery control

I. INTRODUCTION

Recently, photovoltaic (PV) power-generation systems are increasingly important and prevalent in distribution generation systems. A conventional centralized PV array is a serial connection of Numerous panels to obtain higher DC-link voltage for main electricity through a DC-AC inverter Unfortunately, once there is a partial shadow on some panels, the system's energy yield Becomes significantly reduced. An AC module is a micro inverter configured on the rear bezel of a PV panel this alternative solution not only immunizes against the yield loss by shadow effect, but also provides flexible installation options according to the user's budget Many prior research work shave proposed a single-stage DC-AC inverter with fewer components to fit the dimensions of the bezel of the AC module, but their efficiency levels are lower than those of conventional PV inverters. The

power capacity range of a single PV panel is about 100 W to 300 W, and the maximum power point (MPP) [2] voltage range is from 15 V to 40 V, which will be the input voltage of the AC module; in cases with lower input voltage, it is difficult for the AC module to reach high efficiency. However, employing a high step-up DC-DC converter in the front of the inverter improves power-conversion efficiency and provides a stable DC link to the inverter. When installing the PV generation system during daylight, for safety reasons, the AC module outputs zero voltage shows the solar energy through the PV panel and micro inverter to the output terminal when the switches are off. When a worker is installing the AC module, this potential difference could pose hazards to the human body or facilities. A floating active switch is designed to isolate the DC current from the PV panel, for when the AC module is off-grid as well as in then on-operating condition. This isolation ensures the operation of the internal components without any residential energy being transferred to the output or input terminals, which could be un safe. The micro inverter includes DC-DC boost converter, DC-AC inverter with control circuit [1]. The DC-DC converter requires large step-up conversion from the panel's low voltage to the voltage level of the application. Previous research on various converters for high step-up applications has included analyses of the switched-inductor and switched-capacitor types; transformer less switched-capacitor type the voltage-lift type the capacitor-diode voltage multiplier and the boost type integrated with a coupled inductor , these converters by

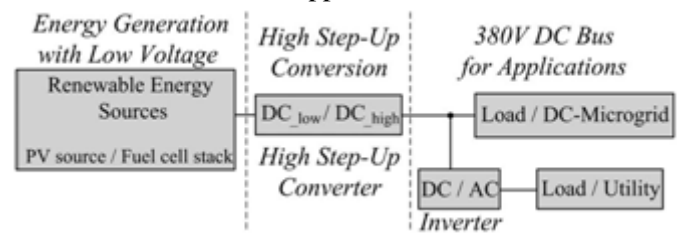
Cite this article as: J Uday Venkatesh, S.J.V Prakesh & L Vijay, "Design of Interleaved Converter with Adaptive SOC Control", International Journal & Magazine of Engineering, Technology, Management and Research, Volume 6 Issue 2, 2019, Page 84-92.

increasing turns ratio of coupled inductor obtain higher voltage gain than conventional boost converter. Some converters successfully combined boost and fly back converters, since various converter combinations are developed to carry out high step-up voltage gain by using the coupled-inductor technique. The efficiency and voltage gain of the DC-DC boost converter are constrained by either the parasitic effect of the power switches or the reverse-recover issue of the diodes. In addition, the equivalent series resistance (ESR) [3] of the capacitor and the parasitic resistances of the inductor also affect overall efficiency. Use of active clamp technique not only recycles the leakage inductor's energy but also constrain the voltage stress across the active switch, however the tradeoff is higher cost and complex control circuit. By combine active snubber, auxiliary resonant circuit, synchronous rectifiers, or switched-capacitor-based resonant circuits and so on, these techniques made active switch into zero voltage switching (ZVS) or zero current switching (ZCS) operation and improved converter efficiency. However, when the leakage-inductor energy from the coupled inductor can be recycled, the voltage stress on the active switch is reduced, which means the coupled inductor employed in combination with the voltage-multiplier or voltage-lift technique successfully accomplishes the goal of higher voltage gain.

The proposed converter, is comprised of a coupled inductor $T1$ with the floating active switch $S1$. The primary winding $N1$ of a coupled inductor $T1$ is similar to the input inductor of the conventional boost converter, and capacitor $C1$ and diode $D1$ receive leakage inductor energy from $N1$. The secondary winding $N2$ of coupled inductor $T1$ is connected with another pair of capacitors $C2$ and diode $D2$, which are in series with $N1$ in order to further enlarge the boost voltage. The rectifier diode $D3$ connects to its output capacitor $C3$. The proposed converter has several features: 1) the connection of the two pairs of inductors, capacitor and diode give a large step-up voltage-conversion ratio; 2) the leakage-inductor energy of the coupled inductor can be recycled, thus increasing the efficiency; and the voltage stress across

the active switch is restrained; and 3) the floating active switch efficiently isolates the PV panel energy during non-operating conditions, which enhances facility and human safety.

Hybrid electric vehicles have recently achieved significant market penetration and stimulated a great amount of research work. Cost-effective high-efficiency integrated power-electronic modules are one of the key elements toward making practical electric propulsions to control the electric-drive motors. The reliability of these power modules is of paramount importance for the commercial success of various types of electric vehicles. Electric-drive trains, due to their wide dynamic range of operation and diverse, impose a stringent reliability requirement on the power modules than any other industrial motor-control applications [4].



As above fig, a typical power module has hundreds of wire bonds and numerous solder joints, which are subject to thermo mechanical stress and fatigue caused by unavoidable power dissipation in the module. The reliability of power semiconductor Modules has been a concern for many industrial Systems, particularly for the railway-traction applications in Europe and Japan, since their market introduction in early 1990s. Module failures are reported in literature both during power-cycling testing and in field usage. Wire-bond lift-off and cracks at silicon-substrate or substrate-base plate solder joints have been identified as the main failure mechanisms. Different operation conditions of the inverters result in varied inverter-phase current and power dissipation. This results in thermo mechanical stress and fatigue. Power modules can and will fail, given enough stress and time. However, power modules usually go through a gradual degradation process before catastrophic failure occurs. The degradation process shows some early symptoms on

the state of health (SoH) of these power modules, including an increase in forward on-voltage, leakage current, thermal impedance, and, possibly, small signal Impedance and noise level. The purpose of this paper is to develop an online diagnostic and prognostic system in electric, hybrid electric, and fuel cell vehicles to warn the driver of potential failure of the power-electronic modules. Online diagnostics and condition. Monitoring was used in induction and brushless dc motors, as well as internal combustion engines. Yet, no work was reported to apply this approach in monitoring the SoH of power modules. In this paper, we first conducted a parametric investigation of power-module degradation processes. A computer-controlled stress test system was developed. Parametric measurement was taken periodically during the power-module stress testing. The measurement results were then analyzed to identify early warning signatures, which were used to provide onboard prognostic capability to monitor the SoH of power modules. Due to the complexity of deterioration mechanisms and the widespread parameter distribution of power modules, we have developed a practical algorithm to implement the prognostic function, to judge whether a power module is on the verge of failing or in a good condition. The algorithm has been verified with extensive Simulink modeling [5].

In the past century, global surface temperatures have increased at a rate near $0.6\text{ }^{\circ}\text{C}/\text{century}$ because of global warming caused by effluent gas emissions and increases in CO_2 levels in the atmosphere. The problems with energy Supply and use are related not only to global warming but also to such environmental concerns as air pollution, acid precipitation, ozone depletion, forest destruction, and radioactive substance emissions. To prevent these effects, some potential solutions have evolved including energy conservation through improved energy efficiency, a reduction in fossil fuel use and an increase in environmentally friendly energy supplies. Recently, energy Generated from clean, efficient and environmentally-friendly sources has become one of the major challenges for engineers and scientists. Among them, the photovoltaic (PV)

generation system has received great attention in research because it appears to be one of the possible solutions to the environmental problem.

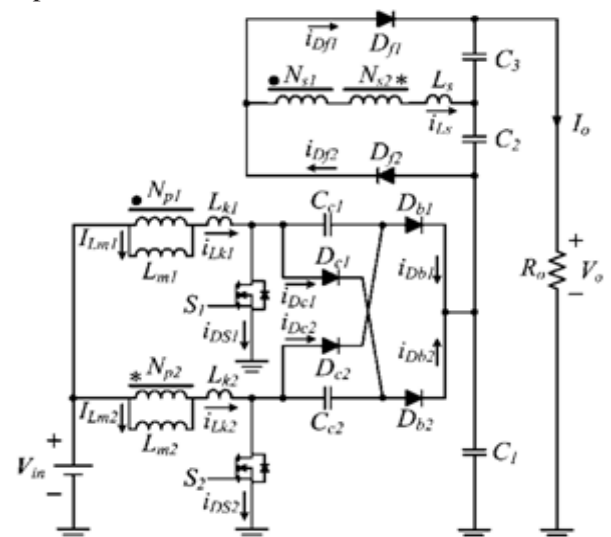
Recently, dc–dc converters with high voltage gain have become usually required in many industrial applications such as the front-end stage for clean-energy sources, the dc back-up energy system for uninterruptible power supply, high-intensity discharge lamps for automobile headlamps, and telecommunication Industry applications. The conventional boost converters cannot provide such a high dc voltage gain, even for an extreme duty cycle. It also may result in serious reverse recovery problem and increase the rating of all devices. As a result, the conversion efficiency is degraded and the electromagnetic interference problem is severe under this situation. To increase the conversion efficiency and voltage gain, many modified step-up converter topologies have been Investigated in the past decades Although voltage clamped techniques are manipulated in the converter design to overcome the severe reverse-recovery problem of the output diode in high-level voltage applications, there still exist overlarge switch voltage stresses and the voltage gain is limited by the turn-on time of the auxiliary switch Wai and Duan investigated a novel coupled-inductor converter strategy to increase the voltage gain of a conventional boost converter with a single inductor, and deal with the problem of the leakage inductor and demagnetization of the transformer in a conventional coupled-inductor-based converter. In this paper, the high step-up converter topology in is introduced to boost and stabilize the output dc voltage of PV modules for the utilization of a dc–ac inverter. Developments in microelectronics and power devices have caused the widespread application of pulse width-modulation(PWM) inverters in industries. The basic mechanism of a PWM inverter is to convert the dc voltage to a sinusoidal ac output through the inverter- LC filter blocks. The performance is evaluated by the total harmonic distortion (THD), the transient response, and the efficiency. Thus, much attention has been paid to the closed-loop regulation of PWM inverters to achieve good dynamic response under

different types of loads in the past decade, e.g., linear control, observer for grid current control, Lyapunov-based control sliding-mode control(SMC) etc. Variable structure control with sliding mode, or SMC, is one of the effective nonlinear robust control approaches since it provides system dynamics with an invariance Property to uncertainties once the system dynamics are controlled in the sliding mode. The insensitivity of the controlled system to uncertainties exists in the sliding mode, but not during the reaching phase, i.e., the system dynamic in the reaching phase is still influenced by uncertainties. Recently some researchers have adopted the idea of total SMC (TSMC) to get a sliding motion through the entire state trajectory, i.e., no reaching phase exists in the control process, so that the controlled system through the whole control processes not influenced by uncertainties. This paper attempts to extend an adaptive TSMC (ATSMC) from the voltage control of a PWM inverter. Up to now, this is the first time that the application of TSMC to the power electronics control is investigated. In general, the output power of a PV module is substantially changed according to different irradiations. For example, in Taiwan, the direction with the maximum average irradiations during the year is South and the corresponding angle of inclinations 23.5° so that many PV modules are installed in this posture. However, the maximum irradiations cannot be captured persistently in this way such that the performance of the PV generation system cannot be improved effectively. Recently, many researchers have made efforts in sun tracking investigations. The conventional sun tracking strategies equip light sensors on the terminals of PV plates. When the feedback signals from light sensors are equal, it means that the PV plate faces the sun and has the maximum irradiation at the corresponding position. Unfortunately, the initial proofreading and correcting of light sensors are time consuming and the device properties are easily varied under different operational conditions. In order to overcome the aforementioned drawbacks, this paper investigates an active sun tracking scheme without light sensors via the property of the open circuit voltage of PV modules proportional to the corresponding irradiation to follow the trail of the

sun. The topic of this paper focuses on the development of a high performance stand-alone PV generation system. It contains three main contents including a high step-up converter, a PWM inverter with ATSMC, and an active sun tracking scheme. First, the active sun-tracking scheme is designed to capture maximum irradiation and powers. Then, the high step-up converter is implemented for converting the captured power from the active sun-tracking scheme to form a stable dc voltage source. In addition, the PWM inverter with ATSMC transfers this dc voltage source from the high step-up converter into an ac voltage source for stand-alone utilization [6].

II INTERLEAVED CONVERTER

The proposed high step-up interleaved converter with a voltage multiplier module is shown in Fig. 2. The voltage multiplier module is composed of two coupled inductors and two switched capacitors and is inserted between a conventional interleaved boost converter to form a modified boost-flyback-forward interleaved structure. When the switches turn off by turn, the phase whose switch is in OFF state performs as a flyback converter, and the other phase whose switch is in ON state performs as a forward converter.



Equivalent circuit of the proposed converter.

At $t=t_0$, the power switch S_2 remains on-state, and other power switch S_1 begins to turn on. The diodes $Dc1$, $Dc2$, $Db1$, $Db2$ and $Df1$ are reversed-biased, as shown in Fig.

2.3 (a). The series leakage inductors L_s quickly releases the stored energy to output terminal via flyback-forward diode $Df2$, and the current through series leakage inductors L_s decreases to zero. Thus, the magnetizing inductor $Lm1$ still transfers energy to secondary side of coupled inductors. The current through leakage inductor $Lk1$ increases linearly, and other current through leakage inductor $Lk2$ decreases linearly.

Mode II [$t1, t2$]:

At $t=t1$, both of the power switches $S1$ and $S2$ remain on-state, and all diodes are reversed-biased, as shown in Fig. 5(b). Both currents through leakage inductors $Lk1$ and $Lk2$, are increase linearly due to charging by input voltage source Vin .

Mode III [$t2, t3$]:

At $t=t2$, the power switch $S1$ remains on-state, and other power switch $S2$ begins to turn off. The diodes $Dc1$, $Db1$ and $Df2$ are reversed-biased, as shown in Fig. 5(c). The energy stored in magnetizing inductor $Lm2$ transfers to secondary side of coupled inductor, and the current through series leakage inductors L_s flows to output capacitor $C3$ via flyback-forward diode $Df1$. The voltage stress on power switch $S2$ is clamped by clamp capacitor $Cc1$ which equals output voltage of boost converter. The input voltage source, magnetizing inductor $Lm2$, leakage inductor $Lk2$ and clamp capacitor $Cc2$ release energy to output terminal, thus $Vc1$ obtains a double output voltage of boost converter.

Mode IV [$t3, t4$]:

At $t=t3$, the current $iDc2$ has naturally decreased to zero due to the magnetizing current distribution, and hence diode reverse recovery losses are alleviated and conduction losses are decreased. Both power switches and all diodes remain previous states except the clamp diode $Dc2$, as shown in Fig. 5(d).

Mode V [$t4, t5$]:

At $t=t4$, the power switch $S1$ remains on-state, and other power switch $S2$ begins to turn on. The diodes $Dc1$, $Dc2$, $Db1$.

Energy Storage:

Electricity is more versatile in use than other types of power, because it is a highly ordered form of energy that can be converted efficiently into other forms. For example, it can be converted into mechanical form with efficiency near 100% or into heat with 100% efficiency. Heat energy, on the other hand, cannot be converted into electricity with such high efficiency, because it is a disordered form of energy in atoms. For this reason, the overall thermal-to-electrical conversion efficiency of a typical fossil thermal power plant is less than 50%.

Disadvantage of electricity is that it cannot be easily stored on a large scale. Almost all electric energy used today is consumed as it is generated. This poses no hardship in conventional power plants, in which fuel consumption is continuously varied with the load requirement. Wind and photovoltaic's (PVs), both being intermittent sources of power, cannot meet the load demand at all times, 24 h a day, 365 d a year.

The present and future energy storage technologies that may be considered for stand-alone wind or PV power systems fall into the following broad categories:

- Electrochemical battery
- Flywheel
- Compressed air
- Superconducting coil

III BATTERY:

The battery stores energy in an electrochemical form and is the most widely used device for energy storage in a variety of applications. There are two basic types of electrochemical batteries:

The *primary battery*, which converts chemical energy into electric energy. The electrochemical reaction in a primary battery is nonreversible, and the battery is discarded after a full discharge. For this reason, it finds applications where a high energy density for one-time use is required.

The *secondary battery*, which is also known as the *rechargeable battery*. The electrochemical reaction in

the secondary battery is reversible. After a discharge, it can be recharged by injecting a direct current from an external source. This type of battery converts chemical energy into electric energy. The internal construction of a typical electrochemical cell is shown in Figure. It has positive and negative electrode plates with insulating separators and a chemical electrolyte in between. The two groups of electrode plates are connected to two external terminals mounted on the casing. The cell stores electrochemical energy at a low electrical potential, typically a few volts. The cell capacity, denoted by C , is measured in ampere-hours (Ah), meaning it can deliver C A for one hour or C/n A for n hours.

The battery is made of numerous electrochemical cells connected in a series-parallel combination to obtain the desired battery voltage and current. The higher the battery voltage, the higher the number of cells required in series. The battery rating is stated in terms of the average voltage during discharge and the ampere-hour capacity it can deliver before the voltage drops below the specified limit. The product of the voltage and ampere-hour forms the watt-hour (Wh) energy rating the battery can deliver to a load from the fully charged condition. The battery charge and discharge rates are stated in units of its capacity in Ah. For example, charging a 100-Ah battery at $C/10$ rate means charging at $100/10 = 10$ A. Discharging that battery at $C/2$ rate means drawing $100/2 = 50$ A, at which rate the battery will be fully discharged in 2 h. The state of charge (SOC) of the battery at any time is defined as the following:

3.1 LEAD-ACID

This is the most common type of rechargeable battery used today because of its maturity and high performance-over-cost ratio, even though it has the least energy density by weight and volume. In a Pb-acid battery under discharge, water and lead sulfate are formed, the water dilutes the sulfuric acid electrolyte, and the specific gravity of the electrolyte decreases with the decreasing SOC. Recharging reverses the reaction, in which the lead and lead dioxide are formed at the negative and positive plates, respectively, restoring the

battery into its originally charged state. The Pb-acid battery comes in various versions. The shallow-cycle version is used in automobiles, in which a short burst of energy is drawn from the battery to start the engine. The deep-cycle version, on the other hand, is suitable for repeated full charge and discharge cycles. Most energy storage applications require deep-cycle batteries. The Pb-acid battery is also available in a sealed "gel-cell" version with additives, which turns the electrolyte into nonspillable gel. The gel-cell battery, therefore, can be mounted sideways or upside down. The high cost, however, limits its use in military avionics.

3.2 NICKEL-CADMIUM

The NiCd is a matured electrochemistry, in which the positive electrode is made of cadmium and the negative electrode of nickel hydroxide. The two electrodes are separated by Nylon™ separators and placed in potassium hydroxide electrolyte in a stainless steel casing. With a sealed cell and half the weight of the conventional Pb-acid, the NiCd battery has been used to power most rechargeable consumer applications. It has a longer deep-cycle life and is more temperature tolerant than the Pb-acid battery. However, this electrochemistry has a memory effect (explained later), which degrades the capacity if not used for a long time. Moreover, cadmium has recently come under environmental regulatory scrutiny. For these reasons, NiCd is being replaced by NiMH and Li-ion batteries in laptop computers and other similar high-priced consumer electronics.

3.3 NICKEL-METAL HYDRIDE

NiMH is an extension of the NiCd technology and offers an improvement in energy density over that in NiCd. The major construction difference is that the anode is made of a metal hydride. This eliminates the environmental concerns of cadmium. Another performance improvement is that it has a negligible memory effect. NiMH, however, is less capable of delivering high peak power, has a high self-discharge rate, and is susceptible to damage due to overcharging. Compared to NiCd, NiMH is expensive at present,

although the price is expected to drop significantly in the future. This expectation is based on current development programs targeted for largescale application of this technology in electric vehicles.

3.4 LITHIUM-ION

The Li-ion technology is a new development, which offers three times the energy density over that of Pb-acid. Such a large improvement in energy density comes from lithium's low atomic weight of 6.9 vs. 207 for lead. Moreover, Li-ion has a higher cell voltage, 3.5 V vs. 2.0 V for Pb-acid and 1.2 V for other electrochemistries. This requires fewer cells in series for a given battery voltage, thus reducing the manufacturing cost.

On the negative side, the lithium electrode reacts with any liquid electrolyte, creating a sort of passivation film. Every time the cell is discharged and then charged, the lithium is stripped away, a free metal surface is exposed to the electrolyte, and a new film is formed. This is compensated for by using thick electrodes or else the battery life would be shortened. For this reason, Li-ion is more expensive than NiCd. In operation, the Li-ion electrochemistry is vulnerable to damage from overcharging or other shortcomings in battery management. Therefore, it requires more elaborate charging circuitry with adequate protection against overcharging.

3.5 LITHIUM-POLYMER

This is a lithium battery with solid polymer electrolytes. It is constructed with a film of metallic lithium bonded to a thin layer of solid polymer electrolyte. The solid polymer enhances the cell's specific energy by acting as both the electrolyte and the separator. Moreover, the metal in solid electrolyte reacts less than it does with a liquid electrolyte.

3.6 ZINC-AIR

The zinc-air battery has a zinc negative electrode, a potassium hydroxide electrolyte, and a carbon positive electrode, which is exposed to the air. During discharge, oxygen from the air is reduced at the carbon electrode

(the so-called air cathode), and the zinc electrode is oxidized. During discharge, it absorbs oxygen from the air and converts it into oxygen ions for transport to the zinc anode. During charge, it evolves oxygen. Good air management is essential for the performance of the zinc-air battery.

3.4 EQUIVALENT ELECTRICAL CIRCUIT:

For steady-state electrical performance calculations, the battery is represented by an equivalent electrical circuit shown in the figure. In its simplest form, the battery works as a constant voltage source with a small internal resistance. The open-circuit (or electrochemical) voltage E_i of the battery decreases linearly with the Ah discharged (Q_d), and the internal resistance R_i increases linearly with Q_d . That is, the battery open-circuit voltage is lower, and the internal resistance is higher in a partially discharged state as compared to the E_0 and R_0 values in a fully charged state.

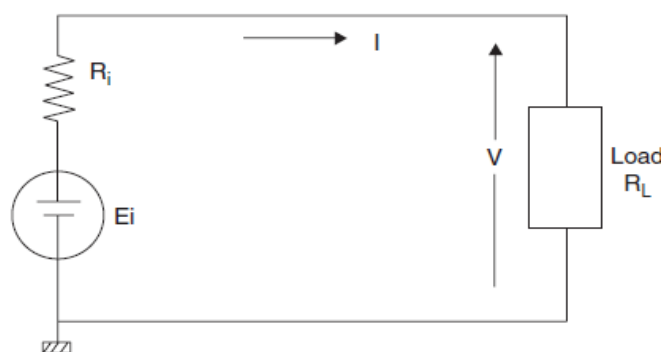


Fig 3.1 Equivalent electrical circuit of battery showing internal voltage and resistance.

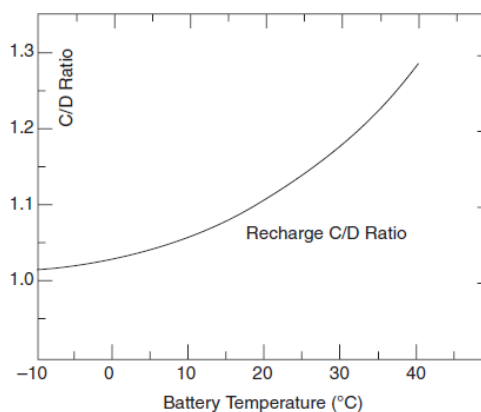


Fig 3.4 Temperature effect on C/D ratio.

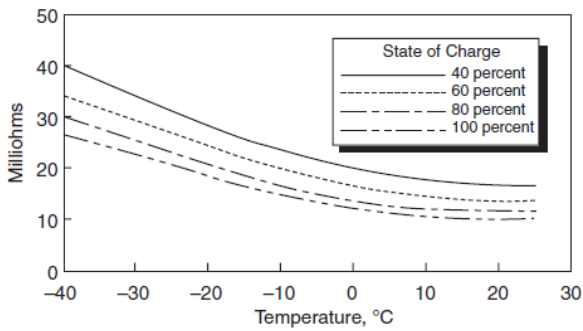
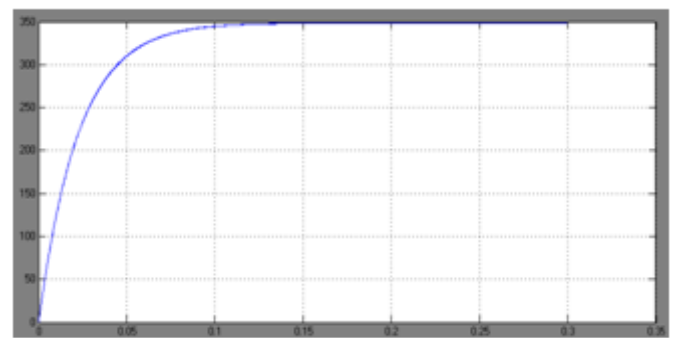
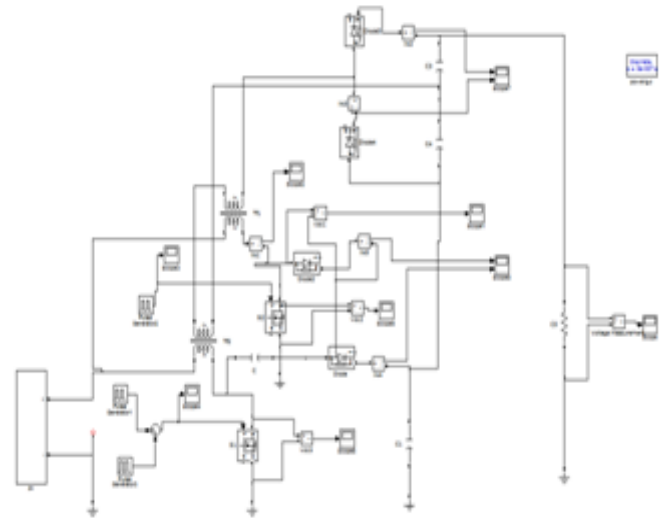
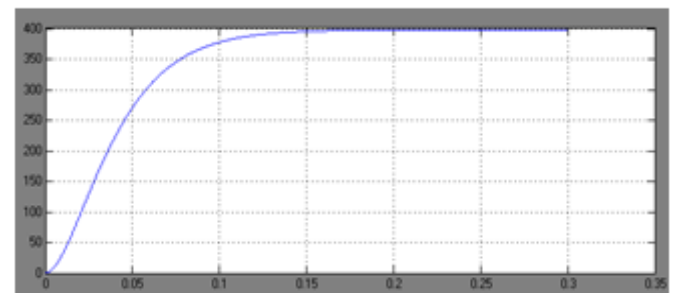
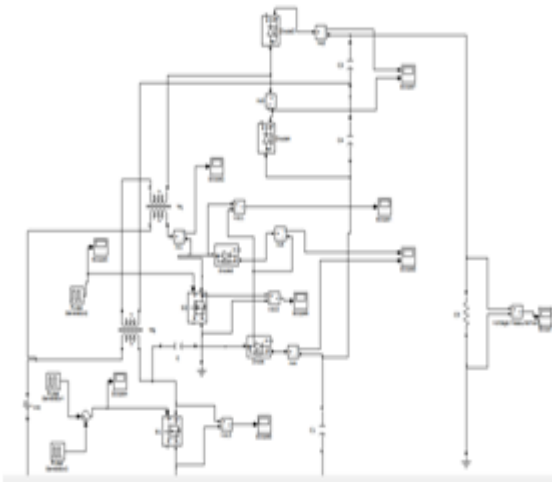


Fig 3.5 Temperature effect on internal resistance in 25-Ah NiCd

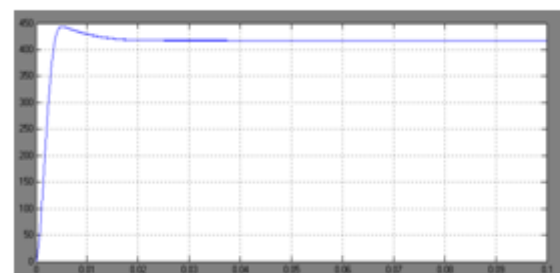
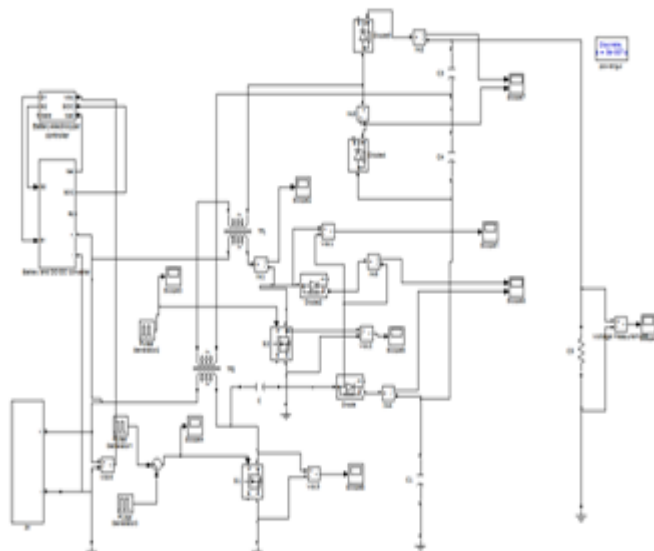
IV Simulation circuits and results



4.1 dc voltage with out solar system



4.2 dc voltage with solar and battery control



4.3 dc voltage without solar and battery control

With battery control

CONCLUSION

This paper has presented the theoretical analysis of steady state, related consideration, simulation results, and experimental results for the proposed converter. The proposed converter has successfully implemented an efficient high step-up conversion through the voltage multiplier module. The interleaved structure reduces the input current ripple and distributes the current through each component. In addition, the lossless passive clamp function recycles the leakage energy and constrains a large voltage spike across the power switch. Meanwhile, the voltage stress on the power switch is restricted and much lower than the output voltage (380 V). Furthermore, the full-load efficiency is 96.4% at $P_o = 1000$ W, and the highest efficiency is 97.1% at $P_o = 400$ W. Thus, the proposed converter is suitable for high-power or renewable energy applications that need high step-up conversion. Maximum power output is obtained when we connect battery to the solar system as a back up.

REFERENCES

- [1] J. T. Bialasiewicz, "Renewable energy systems with photovoltaic power generators: Operation and modeling," *IEEE Trans. Ind. Electron.*, vol. 55, no. 7, pp. 2752–2758, Jul. 2008.
- [2] T. Kefalas and A. Kladas, "Analysis of transformers working under heavily saturated conditions in grid-connected renewable energy systems," *IEEE Trans. Ind. Electron.*, vol. 59, no. 5, pp. 2342–2350, May 2012.
- [3] Y. Xiong, X. Cheng, Z. J. Shen, C. Mi, H. Wu, and V. K. Garg, "Prognostic and warning system for power-electronic modules in electric, hybrid electric, and fuel-cell vehicles," *IEEE Trans. Ind. Electron.*, vol. 55, no. 6, pp. 2268–2276, Jun. 2008.
- [4] A. K. Rathore, A. K. S. Bhat, and R. Oruganti, "Analysis, design and experimental results of wide range ZVS active-clamped L–L type currentfed DC/DC converter for fuel cells to utility interface," *IEEE Trans. Ind. Electron.*, vol. 59, no. 1, pp. 473–485, Jan. 2012.
- [5] T. Zhou and B. Francois, "Energy management and power control of a hybrid active wind generator for distributed power generation and grid integration," *IEEE Trans. Ind. Electron.*, vol. 58, no. 1, pp. 95–104, Jan. 2011.
- [6] N. Denniston, A. M. Massoud, S. Ahmed, and P. N. Enjeti, "Multiplemodule high-gain high-voltage DC–DC transformers for offshore windenergy systems," *IEEE Trans. Ind. Electron.*, vol. 58, no. 5, pp. 1877– 1886, May 2011.